International Journal of Engineering & Applied Sciences (IJEAS)

Vol.6, Issue 3(2014)12-20

EFFECTS OF PERMEABILITY ON DOUBLE DIFFUSIVE MHD MIXED CONVECTIVE FLOW PAST AN INCLINED POROUS PLATE

Md. Nasir Uddin [a*], *M.M.K. Chowdhury* [b] *and M.A. Alim* [c]

[a,,b,c] *Department of Mathematics, Bangladesh University of Engineering & Technology, Dhaka-1000, Bangladesh*
[*] *E-mail address*: *mnasiruddin07@gmail.com*

Abstract

The influence of permeability of the porous plate on double diffusive MHD mixed convective flow past an inclined porous plate in the boundary layer region has been investigated in this paper. The system of non-linear partial differential equations and their boundary conditions have been developed, and transformed into a set of non-linear ordinary differential equations with the help of similarity transformations. These transformed equations are solved numerically for different values of relevant parameters using Runga-Kutta method with Nachtsheim-Swigert shooting iteration technique. Numerical results are obtained for the velocity, temperature and concentration distributions as well as local skin-friction, local Nusselt number and local Sherwood number, and presented graphically to analyze the effects of permeability parameters of the porous plate and the porous medium, and Eckert number. For some specific values of relevant governing parameters, the numerical result is compared with those available in the literature for validity of numerical results and a comparatively good agreement is reached.

Keywords: Double diffusive; MHD; mixed convection; permeability; inclined porous plate.

1. Introduction

Double diffusive MHD mixed convective flow has attracted the considerable interest of many researchers in last several years due to its important applications in many important environmental and engineering fields with applications. The problems involving MHD are very important in many fields such as magnetic behavior of plasmas in fusion reactors, liquid-metal cooling of nuclear reactors, electromagnetic casting, petroleum industries, geophysical, boundary layer control in aerodynamics, MHD generators, crystal growth, Ship propulsion, Jet printers and so on. Moreover, the possible usage of MHD is largely concerned with the flow, heat and mass transfer characteristics for an electrically conducting fluid as the purpose of thermal production, braking, propulsion and control. An analysis of heat and mass transfer in MHD flow by natural convection from a permeable, inclined surface with variable wall temperature and concentration, taking into consideration the effects of ohmic heating and viscous dissipation is investigated by Chen [1]. Alam [2] studied the thermal-diffusion effects as well as heat generation effects on combined free-forced convection and mass transfer flow over a vertical porous flat plate in a porous medium. Combined effect of viscous dissipation and joule heating on the coupling of conduction and free convection along a vertical plate has been discussed by Alim [3]. MHD mixed convective heat transfer about a semi-infinite inclined plate in the presence of magneto and thermal radiation effects has been examined by Aydin and Kaya [4]. MHD mixed convection boundary layer flow with double diffusion and thermal radiation adjacent to a vertical permeable surface embedded in a porous medium has been investigated by Tak [5]. The author Tak [5] presented the numerical results in tabular form for the transverse magnetic field, thermal radiation and Dufour-Soret parameters. Reddy and Reddy [6] analyzed a steady two-dimensional MHD free convection and mass transfer flow past an inclined semi-infinite vertical surface in the presence of heat generation in a porous medium. In a recent investigation, unsteady MHD thermal diffusive, radiative and free convective flow past a vertical porous plate through nonhomogeneous porous medium has been examined by Raju [7]. Steady incompressible boundary layer flow over a permeable vertical plate in the presence of a chemical reaction and wall suction is investigated by Magodora [8]. Guha and Samanta [9] investigated the effect of thermophoresis on the motion of aerosol particles in natural convective flow on horizontal plates. An unsteady free convective MHD flow of a viscous fluid along a semi-infinite vertical plate embedded in a porous medium is investigated with heat source and thermo diffusion by Anuradha and Priyadharshini [10]. As mentioned above, the permeability effects have not been investigated yet on double diffusive MHD mixed convective flow past an inclined porous plate. So it is more reasonable to analyze the permeability effects on the momentum to explore the impact of the momentum, heat and mass transfer characteristics with a transverse applied magnetic field. Therefore, in the light of above literatures, the aim of the present work is to investigate the effects of permeability parameters of the porous plate f_w, the porous medium K, and the Eckert number Ec on double diffusive MHD mixed convective flow past an inclined porous plate.

2. Mathematical Analysis

Consider two-dimensional double diffusive MHD mixed convective flow along an inclined porous plate which makes an acute angle α to the vertical direction. The physical coordinates (x,y) are chosen such that x is measured from the leading edge in the streamwise direction and y is measured normal to the surface of the plate. The velocity components in the directions of flow and normal to the flow are u and v respectively. A uniform magnetic field B_0 which is applied normal to the direction of flow. The external flow with a uniform velocity U_∞ takes place in the direction of flow, parallel to the inclined plate. It is assumed that T and C are the temperature and concentration of the fluid which are the same, everywhere in the fluid. The plate is maintained at a constant temperature T_w, which is higher than the constant temperature T_∞ of the surrounding fluid and the concentration C_w which is greater than the constant concentration C_∞. The schematic view of flow configuration and coordinates system is shown in Fig. 1.

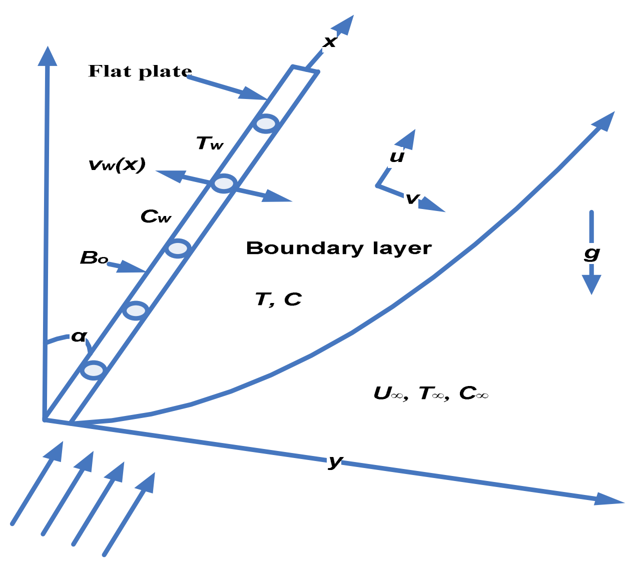

Fig.1: Schematic view of flow configuration and coordinate system

Under the foregoing assumptions, the governing equations in terms of continuity, momentum, energy and concentration equations can be written as:

$$\frac{\partial u}{\partial x}+\frac{\partial v}{\partial y}=0 \tag{1}$$

$$u\frac{\partial u}{\partial x}+v\frac{\partial u}{\partial y}=\nu\frac{\partial^2 u}{\partial y^2}+g\beta(T-T_\infty)\cos\alpha+g\beta^*(C-C_\infty)\cos\alpha-\frac{\sigma B_0^2}{\rho}(u-U_\infty)-\frac{\nu}{K^*}u \tag{2}$$

$$u\frac{\partial T}{\partial x}+v\frac{\partial T}{\partial y}=\frac{k}{\rho c_p}\frac{\partial^2 T}{\partial y^2}+\frac{Q_0}{\rho c_p}(T-T_\infty)+\frac{\sigma B_0^2}{\rho c_p}u^2 \tag{3}$$

$$u\frac{\partial C}{\partial x}+v\frac{\partial C}{\partial y}=D\frac{\partial^2 C}{\partial y^2}-\frac{\partial}{\partial y}\{V_T(C-C_\infty)\} \tag{4}$$

where ν is the kinematics viscosity, g is the acceleration due to gravity, β is the volumetric coefficient of thermal expansion, β^* is the volumetric coefficient of expansion with mass fraction, σ is the electrical conductivity, K^* is permeability of the porous medium, ρ is the density of the fluid, k is the thermal conductivity of the fluid, c_p is the specific heat at constant pressure, Q_0 is the heat generation constant, D is the mass diffusivity and V_T is the thermophoretic velocity.

The appropriate boundary conditions for the flow field, relevant to this investigation are as follows:

$$u=0, v=\pm v_w(x), T=T_w, C=C_w \quad \text{at } y=0 \quad \text{and} \quad u=U_\infty, T=T_\infty, C=C_\infty \quad \text{as } y\to\infty \tag{5.1,5.2}$$

In addition, U_∞ is the free stream velocity and $v_w(x)$ represents the permeability of the porous plate where its sign indicates suction (< 0) or blowing (> 0), subscripts w and ∞ indicate the conditions at the wall and at the outer edge of the boundary layer edge, respectively. In the equation (4) the thermophoretic velocity V_T can be expressed in the following form as:

$$V_T=-\frac{\kappa\nu}{T_{ref}}\frac{\partial T}{\partial y} \tag{6}$$

where T_{ref} is some reference temperature and κ is the thermophoretic coefficient which is defined by Talbot [11]. In order to reduce the number of independent variables and to make the governing differential equations dimensionless, the following dimensionless variables, which defined by Cebeci and Bradshaw [12], are applied:

$$\eta=y\sqrt{\frac{U_\infty}{\nu x}}, \psi=\sqrt{\nu x U_\infty}\,f(\eta), \theta(\eta)=\frac{T-T_\infty}{T_w-T_\infty}, \phi(\eta)=\frac{C-C_\infty}{C_w-C_\infty} \tag{7}$$

where, ψ (x, y) is the stream function defined by $u=\partial\psi/\partial y$ and $v=-\partial\psi/\partial x$, such that the continuity equation (1) is satisfied automatically. In terms of these new variables, the velocity components can be expressed as:

$$u=U_\infty f'(\eta), v=\frac{1}{2}\sqrt{\frac{\nu U_\infty}{x}}(\eta f'-f) \tag{8}$$

where, the prime stands for ordinary differentiation with respect to similarity variable η. Using dimensionless variables, the transformed momentum, energy, and concentration equations together with the boundary conditions can be written as:

$$f''' + \frac{1}{2} ff'' + Gr_t \theta \cos\alpha + Gr_m \phi \cos\alpha - (M + K) f' - M = 0 \tag{9}$$

$$\theta'' + \frac{1}{2} \Pr f \theta' + \Pr Q \theta + Ec \Pr M f'^2 = 0 \tag{10}$$

$$\phi'' + Sc(\frac{1}{2} f - \tau\theta')\phi' - Sc\tau\theta''\phi = 0 \tag{11}$$

with the boundary conditions:

$$f = f_w, f' = 0, \theta = 1, \phi = 1 \quad \text{at} \quad \eta = 0 \quad \text{and} \quad f' \to 1, \theta \to 0, \phi \to 0 \quad \text{as} \quad \eta \to \infty \tag{12.1,12.2}$$

where, Gr_t is the local thermal Grashof number, Gr_m is the local mass Grashof number, M is the magnetic field parameter, K is the permeability parameter, Pr is the Prandtl number, Q is the heat generation parameter, Ec is the Eckert number, Sc is the Schmidt number, τ is the thermophoretic parameter and $f_w = -v_w(x)\sqrt{x/(\nu U_\infty)}$ is the dimensionless wall mass transfer coefficient such that $f_w > 0$ indicates wall suction and $f_w < 0$ indicates wall injection or blowing. The corresponding dimensionless groups that appear in the dimensionless form of governing equations are defined as:

$$\begin{aligned} &Gr_t = \frac{g\beta(T_w - T_\infty)x}{U_\infty^2}, Gr_m = \frac{g\beta^*(C_w - C_\infty)x}{U_\infty^2}, M = \frac{\sigma B_0^2 x}{\rho U_\infty}, K = \frac{\nu x}{K^* U_\infty}, \\ &\Pr = \frac{\nu \rho c_p}{k}, Q = \frac{Q_0 x}{\rho c_p U_\infty}, Ec = \frac{U_\infty^2}{c_p(T_w - T_\infty)}, Sc = \frac{\nu}{D}, \tau = -\frac{\kappa(T_w - T_\infty)}{T_{ref}} \end{aligned} \tag{13}$$

The physical quantities of fundamental interest of heat and mass transfer are the local friction factor in terms of the local skin friction coefficient, the local heat transfer in terms of the local Nusselt number and the local mass transfer coefficients in terms of the local Sherwood numbers, respectively. By employing definition of wall shear stress $\tau_w = \mu(\partial u/\partial y)_{y=0}$ along with Fourier's law $q_w = -k(\partial T/\partial y)_{y=0}$ and Fick's law $J_s = -D(\partial C/\partial y)_{y=0}$, the local skin-friction coefficient is $C_f = 2\mathrm{Re}^{-1/2} f''(0)$, the local Nusselt number is $N_u = -2\mathrm{Re}^{1/2}\theta'(0)$ and the local Sherwood number is $S_h = -2\mathrm{Re}^{1/2}\phi'(0)$, where $\mathrm{Re}_x = xU_\infty/\nu$ is denoting the local Reynolds number.

3. Solution Procedures

In order to solve the system of nonlinear ordinary differential equations (9), (10) and (11), along with the boundary conditions (12.1) and (12.2), we reduce it into initial value problem using Nachtsheim-Swigert shooting iteration technique, and then solve numerically by sixth order Runge-Kutta initial value solver. Due to better numerical results, the sixth order Runge-Kutta initial value method has been used to solve transformed nonlinear ordinary differential equations. In a shooting method, the unspecified initial condition at the terminal point of the interval is assumed, and the differential equation is then integrated numerically as an initial value problem to the terminal point. There are three asymptotic boundary conditions in equation (12) and hence three unknown surface conditions $f''(0), \theta'(0)$ and $\phi'(0)$. The outer boundary conditions may be functionally represented in the initial value method and Nachtsheim-Swigert iteration techniques as

$$\Phi_j(\eta_{\max}) = \Phi_j(f''(0), \theta'(0), \phi'(0)) = \delta_j; \; j = 1, 2, ..., 6 \tag{13}$$

where, $\Phi_1 = f', \Phi_2 = \theta, \Phi_3 = \phi, \Phi_4 = f'', \Phi_5 = \theta', \Phi_6 = \phi'$

The last three represent the asymptotic convergence criteria and choosing as $f'' = g_1, \theta' = g_2$ and $\phi' = g_3$. Now expending equations (13) in a first order Taylor series yield

$$\Phi_j(\eta_{\max}) = \Phi_{j,c}(\eta_{\max}) + \sum_{1}^{3} \frac{\partial \Phi_j}{\partial g_i} \Delta g_i = \delta_j,\ j = 1, 2, ..., 6 \quad (14)$$

where subscript 'c' indicates the value of function at $(\eta_{\max})$ determined from the integration. Consider $E = \sum_{j=1}^{6} \delta_j^2$ and differentiating E with respect to $g_i (i = 1, 2, 3)$, then obtained

$$\sum_{j=1}^{6} \delta_j \frac{\partial \delta_j}{\partial g_i} = 0 \quad (15)$$

Substituting equation (14) in (15) and then obtained,

$$\sum_{k=1}^{3} a_{ik} \Delta g_k = b_i; i = 1, 2, 3 \quad (16)$$

where $a_{ik} = \sum_{j=1}^{6} \frac{\partial \Phi_j}{\partial g_i} \frac{\partial \Phi_j}{\partial g_k}, b_i = -\sum_{j=1}^{6} \Phi_{j,c} \frac{\partial \Phi_j}{\partial g_i}; i, k = 1, 2, 3$

Using Cramer rules in equation (16), then obtained the missing values of g_i as $g_i = g_i + \Delta g_i$. Now the reduced initial value problem solves numerically using sixth order Runge-Kutta initial value method. The numerical methods are described in details, referring to Nachtsheim and Swigert [13]. For the accuracy of the numerical results, the present investigation is compared with the previous investigation by Reddy and Reddy [6] as shown in Fig. 2 while Gr_t = 2.0, Gr_m = 2.0, M = 0.5 (only for coefficient of f' otherwise M = 0.0), Q = 0.5, K = 0.5, $\alpha = 30^0$, Pr = 0.71, Ec = 0.0, f_w = 0.0, Sc = 0.6 and τ = 0.0.

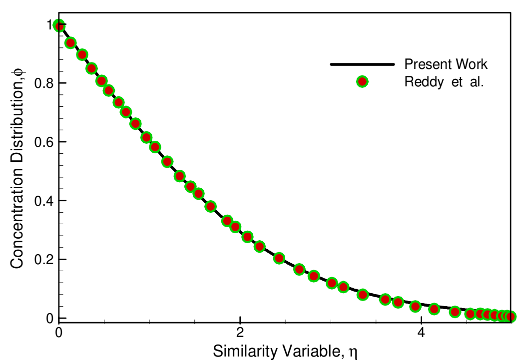

Fig. 2: Comparison of Concentration Distribution

It is observed that the present result is in good agreement with that of Reddy and Reddy [6]. This favorable comparison leads confidence in the numerical results to be reported in the next sections.

4. Results and discussion

The formulation of the problem that accounts for the effects of permeability of porous plate, magnetic field and Eckert number on the flow field is examined and discussed in the preceding sections. This enables to carry out the numerical calculations using different value of various physical parameters for the velocity, temperature and concentration distributions across the boundary layer, as well as the local skin friction coefficient, the local Nusselt number and the local Sherwood numbers at the wall, respectively. The following set of considered values for the relevant parameters in the numerical solutions were adopted, unless otherwise stated; $Gr_t = 0.87$, $Gr_m = 0.87$, $M = 0.001$, $Q = 0.50$, $K = 0.01$, $\alpha = 30^0$, $\Pr = 0.71$, $f_w = 0.50$, $Sc = 0.60$, $\tau = 0.10$ and $U_\infty / \nu = 1.0$. The values of Prandtl and Schmidt numbers are taken to be 0.71 and 0.78 which are corresponding physically to air and ammonia, respectively.

The influence of the permeability parameter f_w (f_w = -1.00 for injection, 0.00 for neither injection nor suction and 1.00 for suction) on the velocity, temperature and concentration distributions as well as the local skin friction coefficient, the local Nusselt number, and the local Sherwood number are presented in Figs. 3(a) - 3(c) and 4(a) – 4(c), keeping other parameters of the flow field constant. It is observed from Fig. 3(a) that, the velocity of the flow field decreases with the increase of permeability of the porous plate. This is because of the fact that, as the permeability through the plate increases, then an opposite fluid velocity which is normal to the direction of the flow, acts through the plate. Therefore, the velocity of the flow field decreases as the permeability of the porous plate increases. With regards to the temperature distribution in Fig. 3(b), it is found that in presence of the fluid suction, the temperature of the flow field decreases as the plate is cooled down due to fluid suction through the plate increases. However, the temperature of the flow field increases as fluid injection through the plate increases. Because of, when the fluid injection through the plate increases, the heat transfer from wall to the fluid increases. On the basis of the concentration distribution in Fig. 3(c), it is seen that the concentration of the flow field at all points decreases as the fluid suction increases, because the larger fluid passing through the plate. But, the concentration of the flow field at all points increases as the fluid injection increases, because the larger fluid coming through the plate within the flow field.

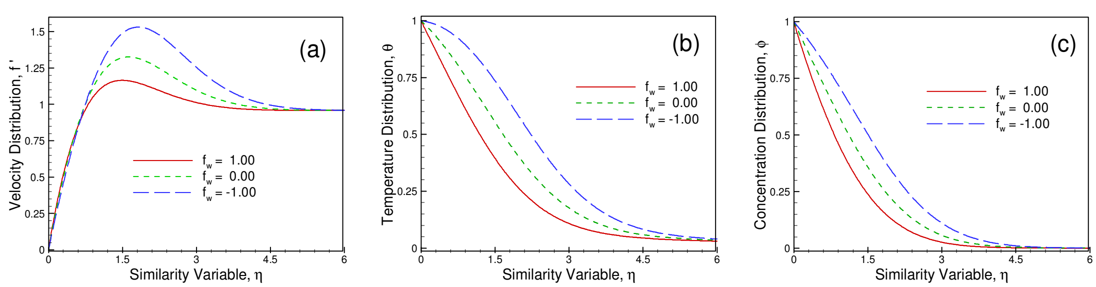

Figs. 3: Representative (a) velocity; (b) temperature; (c) concentration distributions for different values of Permeability parameter of porous plate f_w

Figures 4(a) - 4(c) depict the local skin friction coefficient, the local Nusselt number, and the local Sherwood number at the wall. The local skin friction coefficient C_f increases as the fluid suction increases causing the viscosity of the flowing fluid increases at the wall and inversely for injection, which is observed in Fig. 4(a). On the other hand both the local Nusselt number and the local Sherwood number increase with the increase of fluid suction parameter due to increase in temperature and concentration difference respectively, which are observed in Fig. 4(b) and Fig. 4(c) and inversely for injection. The effect of the permeability parameter of the porous medium K (K = 0.01, 0.03 and 0.05) on the velocity and temperature distributions as well as the local skin friction coefficient and the local Nusselt number are displayed in Figs. 5(a) - 5(b) and Figs 6(a) – 6(b), keeping other parameters of the flow field fixed. On the basis of the velocity distribution in Fig. 5(a), it is seen that the velocity of the flow field within the velocity boundary layer decreases as the permeability of the porous medium increases. Also the velocity boundary layer thickness is found to decrease as growing in the permeability of the porous medium parameter. An observation of the temperature distribution is in Fig. 5(b), the temperature and the thermal boundary layer thickness of the flow field increase due to increase in the permeability of the porous medium parameter. Figs. 6(a) and 6(b) show the influence of permeability of the porous medium on the local skin friction coefficient and the local Nusselt number at the wall. In Figs. 6(a) and 6(b), it is found that both the local skin friction coefficient and the local Nusselt number decrease with the increase of permeability parameter of the porous medium. The variation of velocity and temperature under the influence of Eckert number *Ec* are shown in Figs. 7(a) and 7(b).

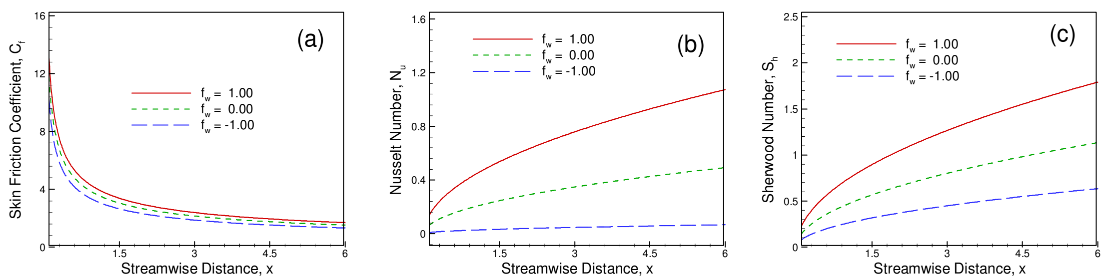

Figs. 4: Effects of Permeability parameter of porous plate f_w on (a) local skin friction coefficient; (b) local Nusselt number; (c) local Sherwood number at the wall

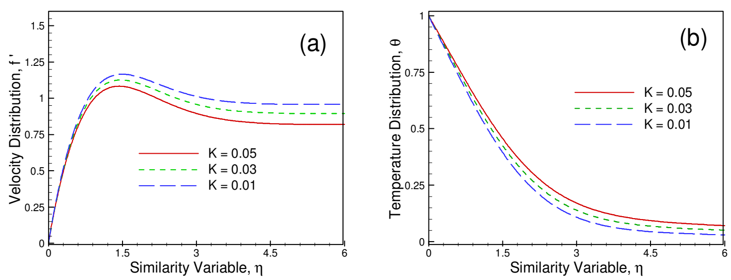

Figs.5: Representative (a) velocity; (b) temperature distributions for different values of permeability parameter of porous medium *K*

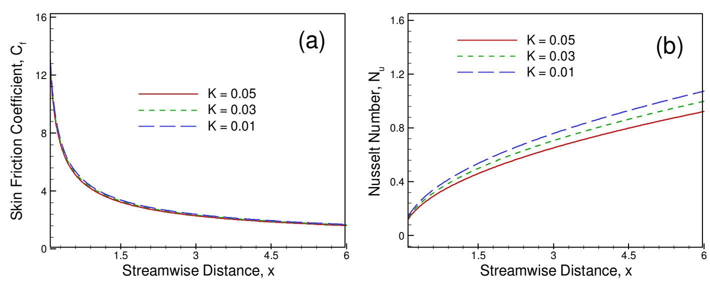

Figs. 6: Effects of permeability parameter of porous medium *K* on (a) local skin friction coefficient; (b) local Nusselt number at the wall

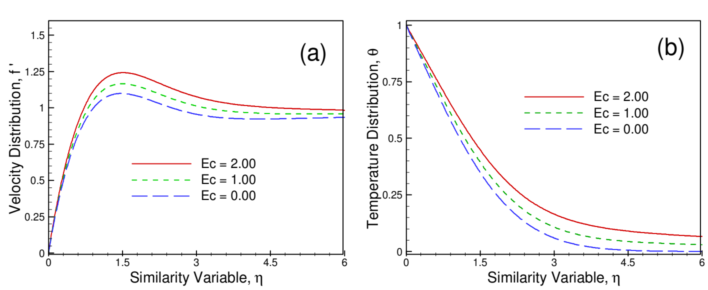

Figs. 7: Representative (a) velocity; (b) temperature distributions for different values of Eckert number *Ec*

From these figures, it is observed that the increase in the values of Eckert number *Ec* tends to increases the momentum and thermal boundary layers, which in turn increasing the velocity and temperature of the flow field. For different values of the Eckert number *Ec,* the local skin-friction coefficient and the local Nusselt number are plotted in Figs. 8(a) and 8(b). It is noted that as the Eckert number *Ec* increases, the local skin-friction coefficient increases, whereas the local Nusselt number decreases.

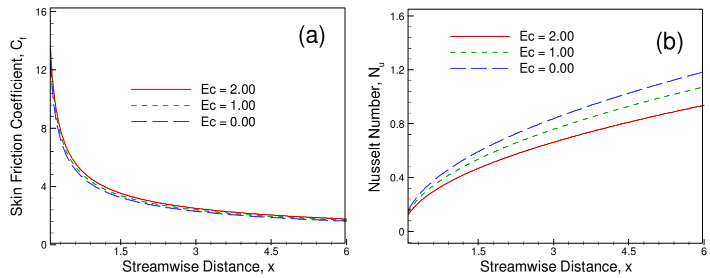

Figs. 8: Effects of Eckert number *Ec* on (a) local skin friction coefficient; (b) local Nusselt number at the wall

5. Conclusions

A mathematical model for double diffusive MHD mixed convective flow past an inclined porous plate, in presence of a transverse uniform magnetic field and suction or injection has been developed and investigated numerically. The numerical results are presented for the effects of permeability parameters of the porous plate f_w , the porous medium *K*, and the Eckert number *Ec* on the flow field. From the present numerical investigation, the following conclusions can be drawn as:

- Fluid suction has the effect to decrease the velocity, temperature and concentration of the flow field whereas increase the local skin friction coefficient, the local Nusselt number and the local Sherwood number, inversely for injection.
- Increases in the permeability of the porous medium, the fluid velocity decreases whereas the temperature increases. On the other hand, the local skin friction coefficient changes insignificantly but the local Nusselt number decreases significantly with the increase of Permeability of porous medium.
- Both the velocity and the temperature of the flow field increase significantly with the increase of Eckert number. Moreover the local skin friction coefficient increases whereas the local Nusselt number decreases due to increase of Eckert number.

References

[1] Chen, C.-H., Yunlin and Taiwan, Heat and mass transfer in MHD flow by natural convection from a permeable, inclined surface with variable wall temperature and concentration, *Acta Mechanica*, 172, pp. 219-235, 2004.
[2] Alam, M.S., Rahman, M.M. and Samad, M.A., Numerical Study of the Combined Free-Forced Convection and Mass Transfer Flow Past a Vertical Porous Plate in a Porous Medium with Heat Generation and Thermal Diffusion, *Nonlinear Analysis: Modeling and Control*, Vol. 11, No. 4, pp. 331-343, 2006.
[3] Alim, M.A, Alam, M.M., Addullah-Al-Mamun and Hossain, B., Combined effect of viscous dissipation and joul heating on the coupling of conduction and free convection along a vertical plate, *International Communications in Heat and Mass Transfer*, Vol. 35, pp. 338-346, 2008.

[4] Aydin, O. and Kaya, A., MHD mixed convective heat transfer flow about an inclined plate, *Heat Mass Transfer*, Vol. 46, pp. 129-136, 2009.
[5] Tak, S.S., Khan, A. and Mathur, R., MHD mixed convection boundary layer flow with double diffusion and thermal radiation adjacent to a vertical permeable surface embedded in a porous medium, *African Journal of Mathematical Physics*, Vol. 8, pp. 67-77, 2010.
[6] Reddy, M.G. and Reddy, N.B., Mass transfer and Heat Generation Effects on MHD Free Convection Flow past an Inclined Vertical Surface in a Porous Medium, *J. of Applied Fluid Mechanics*, Vol. 4, No. 3, Issue 1, pp. 7-11, 2011.
[7] Raju, K.V.S., Raju, M.C., Venkataramana, S. and Raju, G.S.S., Unsteady MHD thermal diffusive, radiative and free convective flow past a vertical porous plate through nonhomogeneous porous medium, *International Journal of Advancements in Research & Technology*, Vol. 2, Issue 7, July-2013.
[8] Magodora, M., Basira, K. and Sibanda, P., Double diffusive heat and mass transfer over a vertical plate in the presence of wall suction and chemical reaction, *International Journal of Scientific and Research and Publications*, Vol. 03, Issue 11, pp. 01-09, November 2013.
[9] Guha, A. and Samanta, S., Effect of thermophoresis on the motion of aerosol particles in natural convective flow on horizontal plates, *International Journal of Heat and Mass Transfer*, Vol. 68, pp. 42-50, 2014.
[10] Anuradha, S. and Priyadharshini, P., Heat and mass transfer on unsteady MHD free convective flow pass a semi-infinite vertical plate with Soret effect, *The International Journal of science & Technoledge*, Vol. 02, Issue 04, pp. 328-337, April 2014.
[11] Talbot, L., Cheng, R.K., Schefer, R.W. and Willis, D.R., Thermophoresis of particles in a heated boundary layer, *J. of fluid Mechanics*, Vol. 101, Part 4, pp. 737-758, 1979.
[12] Cebeci, T. and Bradshaw, P., *Physical and computational aspects of convective heat transfer*, Springer, New York, 1984.
[13] Nachtsheim, P.R. and Swigert, P., *Satisfaction of asymptotic boundary conditions in numerical solution of systems of nonlinear equations of boundary-layer type*, NASA TND 3004, 1965.